Title

Neuronopathy in the Motor Neocortex in a Chronic Model of Multiple Sclerosis

Journal

Journal of Neuropathology & Experimental Neurology, 73(4)

ISSN

0022-3069

Authors

Burns, Travis
Miers, Laird
Xu, Jie
et al.

Publication Date

2014-04-01

DOI

10.1097/nen.0000000000000058

Peer reviewed

Published in final edited form as:
J Neuropathol Exp Neurol. 2014 April ; 73(4): 335–344. doi:10.1097/NEN.0000000000000058.

Neuronopathy in the Motor Neocortex in a Chronic Model of Multiple Sclerosis

Travis Burns, BS[1], **Laird Miers, BS**[1], **Jie Xu, PhD**[1], **Alan Man, PhD**[2], **Monica Moreno, BS**[1,3], **David Pleasure, MD**[1,3], and **Peter Bannerman, PhD**[3,4]

[1]University of California Davis, Department of Neurology, Sacramento, California

[2]University of California Davis, Department of Biomedical Engineering, Davis, California

[3]Institute for Pediatric Regenerative Medicine, Shriners Hospital for Children, Northern California, Sacramento, California

[4]University of California Davis, Department of Cell Biology and Human Anatomy, Davis, California

Abstract

We provide evidence of cortical neuronopathy in myelin oligodendrocyte glycoprotein-peptid-induced experimental autoimmune encephalomyelitis, an established model of chronic multiple sclerosis (MS). To investigate phenotypic perturbations in neurons in this model, we used apoptotic markers and immunohistochemistry with antibodies to NeuN and other surrogate markers known to be expressed by adult pyramidal layer V somas, including annexin V, encephalopsin and Emx1. We found no consistent evidence of chronic loss of layer V neurons but detected both reversible and chronic decreases in the expression of these markers in conjunction with evidence of cortical demyelination and pre-synaptic loss. These phenotypic perturbations were present in but not restricted to neocortical layer V. We also investigated inflammatory responses in the cortex and subcortical white matter of the corpus callosum (CC) and spinal dorsal funiculus and found that those in the cortex and CC were delayed compared to those in the spinal cord. Inflammatory infiltrates initially included T cells, neutrophils and Iba1-positive microglia/macrophages in the CC, whereas only Iba1-positive cells were present in the cortex. These data indicate that we have identified a new temporal pattern of subtle, phenotypic perturbations in neocortical neurons in this chronic MS model.

Keywords

Corticospinal neurons; Motor strip; Multiple sclerosis; Neuronopathy

INTRODUCTION

It has been established that chronic disability in multiple sclerosis (MS) patients correlates with central nervous system neuronal dysfunction. This has been demonstrated in spinal

Send correspondence and reprint requests to: Peter Bannerman, Institute for Pediatric Regenerative Medicine, Shriners Hospitals for Children, Northern California, 2425 Stockton Blvd., Sacramento, CA 95817. Telephone: 916-453-2358; Fax: 916-454-2288; pgbannerman@ucdavis.edu.

white matter tracts in MS patients using magnetic resonance spectrometry to detect depletion of neuronal amino acid N-acetyl-aspartate in axons (1–4). Axonal disruption in MS is also supported by immunohistochemical analysis of biopsy and autopsy tissue detecting aberrant expression of axonal markers such as amyloid precursor protein (5–7) and hypophosphorylated epitopes of neurofilament–heavy chain (8, 9). More recently, histopathological studies and new magnetic resonance spectrometry modalities that are sensitive in detecting grey matter (GM) lesions have led to the recognition that MS is both a grey and white matter disease. In combination these studies have detected demyelination (10–13) and atrophy (14–17) within the cortex. Other studies have provided evidence that neuronal loss and axonal transection can occur alongside demyelination in the MS cortex (18, 19).

In chronic MS and the MS model of experimental autoimmune encephalomyelitis (EAE), axons comprising the corticospinal tract (CST) undergo axonopathy (20–24). We therefore sought evidence of whether such axonopathy occurred in conjunction with cortical neuronopathy in layer V neurons of the corticospinal axis. To investigate this we induced EAE with myelin oligodendrocyte glycoprotein peptide (MOGp) (MOGp-EAE) and analyzed neuronal loss/apoptosis and changes in the expression of markers present in the cortical motor strip by immunohistochemistry. Although a number of markers enriched in layer V neurons have been extensively studied during embryonic and early postnatal corticogenesis (e.g. Ctip 2, Fezl crystallin-mu and Emx1), few of these molecules are expressed in the adult neocortex (25–27). Accordingly, primary antibodies to the neuronal marker NeuN as well as to molecules expressed in, but not exclusive to, layer V in the adult motor cortex, including annexin V, encephalopsin and Emx1 were analyzed. NeuN (Fox-3) is a member of the Fox family of RNA splicing factors that is widely expressed in post-mitotic and differentiated neurons (28, 29). Annexin V is a protein associated with membrane reorganization and calcium signaling and is constitutively expressed focally in layer V neurons (30). Encephalopsin is a member of the opsin photoreceptor family of proteins; its neuronal function has yet to be determined. Antibodies to encephalopsin label pyramidal cells in layers IV and V (31). The transcription factor Emx1 is expressed in neural stem cells and neurons during corticogenesis (32, 33), and in differentiated adult cortical neurons where it is mainly localized in pyramidal neurons in cortical layers II/III and V (34, 35). To include both acute and chronic time-points in EAE pathology we analyzed the frontal neocortex of mice harvested on days (D)14, 21, 35 and 100 post-MOGp inoculation.

We found that neuronal loss in the neocortical motor strip in MOGp-EAE was not a major feature of this MS model of MS but we show for the first time that both reversible and chronic perturbations in neuronal phenotype occur in the motor cortex and that they were not restricted to layer V, as per our initial expectation. These perturbations correlated well with phases of cortical demyelination and pre-synaptic loss (as assessed by myelin basic protein [MBP] and synaptophysin immunohistochemistry), rather than inflammatory responses in the underlying white matter of the corpus callosum (CC) and in the dorsal corticospinal tract (dCST).

MATERIALS AND METHODS

Induction of MOGp-EAE

MOGp-EAE was induced in 3-month-old adult male C57BL/6 mice (Jackson Laboratories, Sacramento, CA), by subcutaneous flank inoculation with 300 μg of rodent MOG peptide (amino acids 35–55, New England Peptides, Gardner, MA) in complete Freund's Adjuvant (CFA), as previously described (36), with 1 modification: pertussis toxin (200 ng) was administered intraperitoneally rather than intravenously on D1 and D3. Control mice were inoculated with CFA without MOGp and treated with pertussis toxin. Neurological deficits were scored using the following scale: limp tail or waddling gait = 1; limp tail and waddling gait = 2; single limb paresis and ataxia = 2.5; double limb paresis = 3; single limb paralysis and single limb paresis = 3.5; paralysis of both hind limbs = 4; moribund = 4.5; and death = 5 (36, 37).

Tissue Processing and Immunohistochemistry

Control CFA- and MOGp-treated mice were deeply anesthetized with ketamine (150 mg/Kg)/xylazine(16 mg/kg), then transcardially perfused with phosphate buffered saline (PBS) followed by 4% paraformaldehyde (freshly prepared from 16% paraformaldehyde stock solution, EM Sciences, Hatfield, PA). Brain tissue was removed and post-fixed in fresh fixative for a further 1 to 2 hours at 4°C.

Coronal forebrain brain sections selected for motor strip analysis were taken between bregma coordinates 0.26 and −0.82, which included the primary motor and primary somatosensory-hind limb portions of the motor strip with varying overlap with the secondary motor and primary somatosensory-forelimb regions (38). The region of interest selected for analysis within the cortex is depicted in Figure 1A. This area excluded the cingulate cortex in more rostral sections and the retrosplenial dysgranular and granular cortex in more caudal sections lying adjacent to the longitudinal fissure.

To prepare brain tissue for cryosectioning, samples were cryoprotected in 30% sucrose in PBS for 48 to 72 hours at 4°C prior to embedding in OCT mounting medium and frozen in cryomolds with dry-ice-cooled 95% ethanol. Twenty-μm-thick cryosections were cut using a Leica cryostat (model CM1950) and collected on poly-lysine-coated glass slides. Immunolabeling with antibodies to Ly6G, CD3, Iba1 and activated caspase 3 (Table) and TUNEL (terminal deoxynucleotidyl transferase-mediated dUTP nick end labeling) histochemistry (39) were performed on cryosections. All other immunostaining was performed using paraffin embedded tissue (Table).

For paraffin embedding, tissue was placed into tissue and biopsy cassettes (Fisher Scientific, USA) and processed using a Shandon Excelsior Tissue Processor (ThermoFisher, Waltham, MA). Thirty-μm-thick sections were cut using a Rotary Microtome (HM 355 S-2, Microm International GmbH, Walldorf, Germany) for histological and immunofluorescence studies and stereology analysis. Paraffin sections were deparaffinized with xylene and descending alcohols and subjected to antigen retrieval with sodium citrate, pH 6.0. To increase penetration of primary antibodies into the sections, slides were pre-incubated in blocking solution composed of either 10% donkey or goat serum diluted in minimum essential

medium containing 15 mM HEPES, 0.05% sodium and 0.1% tween-20 for 1 hour. This blocking solution was also used as a diluent for both primary and secondary antibody incubations. Sections were incubated with primary antibodies for 48 hours at 4°C and secondary antibodies for 1 hour at room temperature with 3 5-minute PBS washes between all steps.

When a mouse monoclonal antibody was used as a primary antibody, tissue sections were pretreated with donkey or goat anti-mouse Fab fragments (260 μg/ml, Jackson Immunoresearch Labs, West Grove, PA) to block binding to endogenous mouse immunoglobulins. Detection of primary antibody binding was performed using species-specific fluorochrome-conjugated second antibodies (Jackson Immunoresearch). When the biotin/streptavidin secondary detection system was used to enhance the sensitivity of immunofluorescence detection, sections were also pre-treated with the biotin/streptavidin blocking kit as per the manufacturer's instructions (Vector Laboratories, Burlingame, CA). Following secondary detection, cryostat sections were post-fixed with −20°C methanol and counterstained with DAPI. The TUNEL assay was performed using a commercially available Neuroapototic Kit supplied by FD Neurotechnologies, Inc. (Columbia, MD). The assay was performed as per the manufacturer's instructions with the exception that streptavidin-conjugated Daylight 594 (Jackson ImmunoResearch) was used as a fluorescent substitute for peroxidase/DAB chromogen detection. The procedure also included the use of positive control slides containing brain tissue with striatal apoptotic neurons (FD Neurotechnologies, Inc.). Following the TUNEL assay, slides were counterstained with Neurotrace 640/ reagent (Life Technologies, Grand Island, NY, diluted 1:40) as a fluorescent alternative to Nissl staining.

Confocal Microscopy

Immunolabeled sections were imaged using a Nikon upright microscope (Nikon Eclipse 90i, Nikon Instruments, Melville, NY) coupled to an A1 laser scanning confocal head with a multi-laser launch coupled through a single mode fiber. Confocal images were processed using Nikon NIS-Elements software.

Non-biased Stereology

Quantitation of NeuN, encephalopsin, Emx-1 and annexin V immunolabeled cortical neurons were obtained using a computer interfaced with an Olympus BX61-DSU microscope with a motorized stage, running StereoInvestigator software (version 10, MicrobrightField), as previously described (40). In brief, 30-μm serial paraffin sections were placed individually on slides and every third slide was immunolabeled as described above. Sections (n = 5) were analyzed per animal and 3 animals were used per time-point. Regions of interest in layers 1–4 and 5 were traced at low magnification (4× magnification, NA 0.16), within the motor strip including the primary motor cortex, secondary motor cortex, and primary somatosensory hind limb region (Fig. 1A). Counting was performed using random counting grids (50 × 50 μm) and a 40× objective (NA 1.3). For layers 1–4, counting sites ranged between 23–30 and for layer 5, 14–17 sites were counted. The optical dissector and guard zone were set at 20 and 2 μm, respectively. Cell densities were calculated by dividing the averaged total immunolabeled cell number by the product of counting site

volume × mean number of total sites and correcting the values as cells per cubic mm. The data obtained from this analysis were tested for significance by the Wilcoxon-Mann Whitney test.

Quantitation of Cortical Demyelination and Pre-synaptic Loss Using MBP and Synaptophysin Immunohistochemistry

Seven-μm-thick paraffin sections were immunolabeled with antibodies to MBP and synaptophysin (Table) and stitched optical sections from the S1HL region (Fig. 1A), including layers I through VI (Fig. 1D) from the brains of CFA and MOGp-EAE mice at D14, 21, 35, and 100 post-MOG immunization. Because of the diffuse nature of both MBP and synaptophysin immunolabeling, quantification was performed using integrated fluorescence density measurements using ImageJ version 1.46 (41). Two sections from each of 3 mice per time-point were analyzed.

RESULTS

Absence of Chronic Neuronal Loss Within the Motor Strip in MOGp-EAE

We first focused on using NeuN and activated caspase 3 immunoreactivity and the TUNEL assay to detect neuronal loss/apoptosis in the motor strip of MOGp-EAE mice. Because active spinal cord inflammatory lesions in MOGp-EAE contain many apoptotic cells, this tissue served as a positive control (Fig. 1B, C), in addition to the positive control tissue provided in the Neuroapototic kit. Although we did not detect any evidence of neuronal apoptosis in the motor strip (Fig. 1D, E), we observed an apparent dramatic loss of neurons, as evidenced by significantly reduced NeuN immunolabeling at D14 using conventional fluorescence microscopy. We subsequently employed the biotin/streptavidin system of detection and confocal microscopy to enhance both the sensitivity and resolution of detecting NeuN immunoreactivity. At D14 post-MOGp vaccination there was a significant reduction or even complete loss of NeuN immunoreactivity in the perikarya of neurons in all layers of the motor cortex (Fig. 2B). We then analyzed NeuN expression at different time-points during the course of MOGp-EAE where it became evident that the number of NeuN-positive neurons had recovered to control levels by D100, indicating no neuronal loss in the motor cortex (Figs. 2A–E, 3A).

Reversible and Chronic Neuronopathy in MOGp-EAE

We also analyzed the expression of encephalopsin (Fig. 2F–J) and annexin V (Fig. 2K–O), which were expressed in but not exclusive to layer V neurons. The expression of these markers was also decreased alongside NeuN at D14 (Fig. 2). For both NeuN and encephalopsin expression these changes appeared reversible because levels of expression increased to control levels at D100, whereas expression of annexin V remained low at D100. There was also a substantial second loss of encephalopsin expression at D35 (Fig. 2I).

We then quantified the neuronal expression of NeuN and other markers selectively in layer V and the sum of those markers present in layers I/II/III and IV using unbiased stereology. These data support the semi-quantitative profile shown in Figure 2 and further show that there was no loss of NeuN-positive neurons in layer V at D100 despite earlier decreases in

NeuN immunoreactivity. There were significant decreases in the number of encephalopsin-, annexin V- and Emx1-positive neurons at D14, respectively (Fig. 3B–D); encephalopsin expression also decreased dramatically at D35 prior to recovering to control levels at D100 (Fig. 3B). Annexin V immunolabeling transiently recovered at D21 prior to decreasing at D35 through D100 (Fig. 3C). Emx1 expression diminished chronically from D14 onwards (Fig. 3D). Figure 3 also demonstrates that perturbations in neuronal phenotype were not restricted to layer V neurons but were also present in other layers (I–IV) of the cortical motor strip.

Inflammatory Responses in Layer V Cortex, Subcortical White Matter and the Dorsal Funiculus

The presence and extent of inflammatory infiltrates associated with meningeal blood vessels in the neocortex were considerably less than those in the spinal cord (Fig. 4). Most inflammatory cells in the cortical region were present in the subcortical white matter, i.e. the CC (Fig. 4H), and their presence was delayed compared to the development of inflammatory lesions in the spinal cord white matter (Fig. 4B). Peak levels of Ly6G-positive neutrophils and CD3-positive T-lymphocytes were seen in the corpus callosum between D21 and D35 (Fig. 4H, I) vs. D14 and D21 (Fig. 4B, C) in the spinal cord dCST. Notably, neutrophils and T cells were mostly absent in the cortex with Iba1-positive cells constituting the main inflammatory cell type between D21 and D35 (Fig. 4M, N).

Cortical Demyelination and Pre-synaptic Loss

In view of the lack of correlation between the transient phases of neuronopathy and inflammatory events in both the white matter of the CC and dCST, we investigated the occurrence of cortical grey matter demyelination and synaptic perturbations, both of which have been described in the GM of MS patients. To this end, we performed immunohistochemistry using antibodies to MBP and synaptophysin to detect demyelination and perturbations in pre-synaptic terminals, respectively. There were significant decreases in both MBP and synaptophysin immunoreactivity at D14 and D35 vs. CFA control and D100 levels of expression with a partial recovery phase at D21 (Fig. 5). These transient changes in MBP and synaptophysin expression match the phasic neuronopathy described above.

DISCUSSION

The last decade and a half has seen a dramatic expansion in our understanding of the involvement of GM pathology in MS. GM pathology has been detected in all MS phenotypes (16, 42). GM lesions may precede the presence of clinical symptoms and the detection of white matter (WM) lesions and correlate with a broader spectrum of neurological symptoms (cognitive and neuropsychiatric symptoms alongside spasticity and other motor deficits) than can be assessed from WM lesion loads alone in MS patients (14, 43–45). Despite these advances the interpretation and correlation of these findings to clinical manifestations is far from complete and straightforward. This is particularly true with regard to the heterogeneity in both clinical and histopathological findings, not only between but also within MS phenotypes. For example, with respect to cortical involvement in patients with chronic MS, Peterson et al reported the presence of occasional apoptotic neurons in

cortical autopsy samples from 11 of 22 MS patients (18). Although these apoptotic profiles were rare, their accumulation over time could result in significant neuronal loss. Because the presence of apoptotic neurons may not be a sufficiently sensitive method for assessing neuronal loss and because neurons may undergo necrotic (non-apoptotic) cell death, it is important to quantify total neuronal numbers in autopsy specimens or during disease progression in MS and EAE models.

Our objective to focus on cortical neuronopathy and in particular layer V neurons in a chronic model of MS was driven by previous findings demonstrating axonopathy in the corticospinal tract of patients with chronic MS (20, 21) and the dCST in EAE mice (22–24).

We were unable to detect any evidence of neuronal apoptosis either by the TUNEL assay or detection of activated caspase 3 immunoreactivity within layer V in MOGp-EAE mice up to 100 days post-MOGp inoculation, a period encompassing both the acute and chronic phases of axonopathy and neuronopathy in the spinal cord. We performed quantitative immunohistochemical analysis to detect potential neuronal loss despite the absence of detectable apoptosis. Our results demonstrate that although there was a window of substantial reduction in cortical NeuN expression, this transient neuronopathy did not equate with detectable neuronal loss in D100 in mice with MOGp-EAE. This result supports the fact that neuronal loss is not a consistent feature of cortical GM pathology in patients with chronic MS (18, 19). However, it should be noted that our results contrast with a previous study using MOGp-EAE in which TUNEL-positive neurons were identified within the cortex (46). One possibility for this discrepancy in results is the fact that the latter authors vaccinated mice twice with MOGp, which may result in a secondary and more robust autoimmune inflammatory and neurotoxic response. Interestingly, in another study it was shown that apoptotic cortical neurons were indeed absent in MOGp-EAE (using a single MOGp injection), but were detectable in an inflammatory model involving focal induction of interleukin-1 expression (47).

A major finding of this study was the existence of both reversible and chronic perturbations in neuronal phenotype, as assessed by decreases in the expression of NeuN, Emx1, encephalopsin and annexin V immunoreactivity. The first phase of neuronopathy occurred during the acute inflammatory phase of MOGp-EAE typified by intense inflammatory infiltrates in WM tracts adjacent to major meningeal blood vessels in the spinal cord. The genesis of these lesions began as early as D7 and peaked by D21 post-MOGp inoculation (23, 48, 49). Within these spinal lesions, neutrophils and CD3-positive T cells initially invaded the WM followed by extensive infiltration with monocytes/macrophages and the activation of parenchymal microglia. By comparison, fewer inflammatory cells were present in the deeper WM tracts, including the dCST. Within the brain, various white matter tracts also became seeded with inflammatory cells (50, 51) (Fig. 4), although submeningeal inflammatory lesions are significantly smaller and less intense compared to those seen in the spinal cord. Our results also show that the appearance of inflammatory infiltrates in the CC is later (D21) than the acute cortical neuronopathy (D14), as well as the submeningeal inflammatory lesions in the spinal cord. Moreover, at D21, the expression levels of NeuN, encephalopsin annexin V and Emx1 recovered to the levels in the CFA control mice in layers I–IV, whereas only annexin V expression recovered in layer V at this time-point.

Also, inflammatory cells in the CC initially included neutrophils, T cells and monocyte/macrophages/microglial cells while in the cortex, Iba1-positive cells with a ramified morphology predominated. Typically, the Iba1-positive cells are classified as activated microglial cells, although we cannot exclude the possibility that they may include macrophages that migrated from the CC and adopted a ramified morphology once in the cortical GM. These results are consistent with previous histopathological studies showing that CD68-positive microglia/macrophage cells are the predominant inflammatory cell type present in both focal and diffuse lesions in the cortex of patients with chronic MS (18, 52, 53).

During the chronic phase of MOGp-EAE (D35–D100), we have previously shown that significant axonopathy occurs in the dCST. While we detected evidence of cortical neuronopathy at D35, the expression of cortical neuronal markers NeuN/encephalopsin and Emx1 returned to control or near control levels by D100. Taken together with our observation that cortical neuronopathy is not restricted to layer V neurons in the motor strip, overall we found no definitive cause and effect relationship between GM and WM pathology during either the acute or chronic phase of MOGp-EAE. These findings are consistent with the notion that in MS, GM and WM pathology can occur independently of each other (10, 14, 45). In marked contrast to these results, we have demonstrated clear evidence that within the cortical GM itself, transient neuronopathy correlates strongly with phasic demyelination and loss of presynaptic terminals at D14 and D35 post-MOGp vaccination (Figs. 2 and 3 vs. Fig. 5). During the acute phase (D14), these synaptic perturbations and demyelination occurred in the absence of obvious microglial cell activation and inflammatory cell infiltration in either the cortical GM and underlying CC (Fig. 4G, L). In a recent study using two-photon microscopy, live recordings of synaptic turnover in layer V of the somatosensory cortex was studied in the pre-symptomatic phase of MOGp-EAE (54). It was found that synaptic turnover increased during this period in the absence of T cells and activated microglia/macrophages. These pre-symptomatic synaptic changes were prevented by peripheral administration of a soluble tumor necrosis factor inhibitor, indicating how cortical GM function might be perturbed by a peripheral cytokine in the absence of local inflammatory cells.

Our results demonstrating demyelination in the MOGp-EAE motor cortex are consistent with numerous reports of cortical GM demyelination. Synaptic perturbations involving loss of synaptophysin have also been described in the cortex of MS patients (55, 56). Further studies will be required to elucidate the ‘cause-effect’ relationships between cortical neuronopathy/demyelination/pre-synaptic loss/ and possible axonopathy in MOGp-EAE.

In summary, this study highlights the occurrence of reversible and chronic phenotypic perturbations in the cell somas of cortical neurons in the motor strip in MOGp-EAE mice, a model of chronic MS. This neuronopathy occurs alongside cortical demyelination and synaptic histopathology. These perturbations may contribute to subtle motor and cognitive deficits. This study also shows that using NeuN immunohistochemistry as a sole indicator of neuronal loss in histopathological studies may be problematic, as a significant reduction in NeuN immunoreactivity could be misinterpreted as neuronal loss. Therefore, we recommend

caution when interpreting reductions in NeuN immunoreactivity as a sole means for quantifying potential neuronal loss, particularly in short-term EAE studies.

Acknowledgments

This work was supported by National Institutes of Health grant RO1 NS025044, National Multiple Sclerosis Society Grant RG4397-A-5, Childrens Miracle Network Grant CMNPB11 and the Shriners Hospitals for Children.

References

1. Bjartmar C, Kidd G, Mörk S, et al. Neurological disability correlates with spinal cord axonal loss and reduced N-acetyl aspartate in chronic multiple sclerosis patients. Ann Neurol. 2000; 48:893–901. [PubMed: 11117546]
2. Davie CA, Barker GJ, Webb S, et al. Persistent functional deficit in multiple sclerosis and autosomal dominant cerebellar ataxia is associated with axon loss. Brain. 1995; 118:1583–92. [PubMed: 8595487]
3. Leary SM, Davie CA, Parker GJ, et al. 1H magnetic resonance spectroscopy of normal appearing white matter in primary progressive multiple sclerosis. J Neurol. 1999; 246:1023–6. [PubMed: 10631633]
4. Lee MA, Blamire AM, Pendlebury S, et al. Axonal injury or loss in the internal capsule and motor impairment in multiple sclerosis. Arch Neurol. 2000; 57:65–70. [PubMed: 10634450]
5. Ferguson B, Matyszak MK, Esiri MM, et al. Axonal damage in acute multiple sclerosis lesions. Brain. 1997; 120:393–9. [PubMed: 9126051]
6. Bitsch A, Schuchardt J, Bunkowski S, et al. Acute axonal injury in multiple sclerosis. Correlation with demyelination and inflammation. Brain. 2000; 123:1174–83. [PubMed: 10825356]
7. Kuhlmann T, Lingfeld G, Bitsch A, et al. Acute axonal damage in multiple sclerosis is most extensive in early disease stages and decreases over time. Brain. 2002; 125:2202–12. [PubMed: 12244078]
8. Trapp BD, Peterson J, Ransohoff RM, et al. Axonal transection in the lesions of multiple sclerosis. New England Journal of medicine. 1998; 338:278–85. [PubMed: 9445407]
9. Trapp BD, Ransohoff R, Rudick R. Axonal pathology in multiple sclerosis: relationship to neurologic disability. Curr Opin Neurol. 1999; 12:295–302. [PubMed: 10499174]
10. Kutzelnigg A, Lucchinetti CF, Stadelmann C, et al. Cortical demyelination and diffuse white matter injury in multiple sclerosis. Brain. 2005; 128:2705–12. [PubMed: 16230320]
11. Albert M, Antel J, Brück W, et al. Extensive cortical remyelination in patients with chronic multiple sclerosis. Brain Pathol. 2007; 17:129–38. [PubMed: 17388943]
12. Bö L. The histopathology of grey matter demyelination in multiple sclerosis. Acta Neurol Scand Suppl. 2009:51–7. [PubMed: 19566500]
13. Kidd D, Barkhof F, McConnell R, et al. Cortical lesions in multiple sclerosis. Brain. 1999; 122:17–26. [PubMed: 10050891]
14. Calabrese M, Rinaldi F, Poretto V, et al. The puzzle of multiple sclerosis: gray matter finds its place. Expert Rev Neurother. 2011; 11:1565–8. [PubMed: 22014135]
15. De Stefano N, Matthews PM, Filippi M, et al. Evidence of early cortical atrophy in MS: relevance to white matter changes and disability. Neurology. 2003; 60:1157–62. [PubMed: 12682324]
16. Roosendaal SD, Bendfeldt K, Vrenken H, et al. Grey matter volume in a large cohort of MS patients: relation to MRI parameters and disability. Mult Scler. 2011; 17:1098–106. [PubMed: 21586487]
17. Dalton CM, Chard DT, Davies GR, et al. Early development of multiple sclerosis is associated with progressive grey matter atrophy in patients presenting with clinically isolated syndromes. Brain. 2004; 127:1101–7. [PubMed: 14998914]
18. Peterson JW, Bö L, Mörk S, et al. Transected neurites, apoptotic neurons, and reduced inflammation in cortical multiple sclerosis lesions. Ann Neurol. 2001; 50:389–400. [PubMed: 11558796]

19. Magliozzi R, Howell OW, Reeves C, et al. A Gradient of neuronal loss and meningeal inflammation in multiple sclerosis. Ann Neurol. 2010; 68:477–93. [PubMed: 20976767]
20. DeLuca GC, Ebers GC, et al. Axonal loss in multiple sclerosis: a pathological survey of the corticospinal and sensory tracts. Brain. 2004; 127:1009–18. [PubMed: 15047586]
21. Ganter P, Prince C, Esiri MM. Spinal cord axonal loss in multiple sclerosis: a post-mortem study. Neuropathol Appl Neurobiol. 1999; 25:459–67. [PubMed: 10632896]
22. Gruppe TL, Recks MS, Addicks K, et al. The extent of ultrastructural spinal cord pathology reflects disease severity in experimental autoimmune encephalomyelitis. Histol Histopathol. 2012; 27:1163–74. [PubMed: 22806903]
23. Soulika AM, Lee E, McCauley E, et al. Initiation and progression of axonopathy in experimental autoimmune encephalomyelitis. J Neurosci. 2009; 29:14965–79. [PubMed: 19940192]
24. Liu Z, Li Y, Zhang J, et al. Evaluation of corticospinal axon loss by fluorescent dye tracing in mice with experimental autoimmune encephalomyelitis. J Neurosci Methods. 2008; 167:191–7. [PubMed: 17919735]
25. Arlotta P, Molyneaux BJ, Chen J, et al. Neuronal subtype-specific genes that control corticospinal motor neuron development in vivo. Neuron. 2005; 45:207–21. [PubMed: 15664173]
26. Greig LC, Woodworth MB, Galazo MJ, et al. Molecular logic of neocortical projection neuron specification, development and diversity. Nat Rev Neurosci. 2013; 14:755–69. [PubMed: 24105342]
27. Molyneaux BJ, Arlotta P, Menezes JR, et al. Neuronal subtype specification in the cerebral cortex. Nat Rev Neurosci. 2007; 8:427–37. [PubMed: 17514196]
28. Kim KK, Adelstein RS, Kawamoto S. Identification of neuronal nuclei (NeuN) as Fox-3, a new member of the Fox-1 gene family of splicing factors. J Biol Chem. 2009; 284:31052–61. [PubMed: 19713214]
29. Dent MA, Segura-Anaya E, Alva-Medina J, et al. NeuN/Fox-3 is an intrinsic component of the neuronal nuclear matrix. FEBS Lett. 2010; 584:2767–71. [PubMed: 20452351]
30. Belgard TG, Marques AC, Oliver PL, et al. A transcriptomic atlas of mouse neocortical layers. Neuron. 2011; 71:605–16. [PubMed: 21867878]
31. Blackshaw S, Snyder SH. Encephalopsin: a novel mammalian extraretinal opsin discretely localized in the brain. J Neurosci. 1999; 19:3681–90. [PubMed: 10234000]
32. Cecchi C, Boncinelli E. Emx homeogenes and mouse brain development. Trends Neurosci. 2000; 23:347–52. [PubMed: 10906797]
33. Schuurmans C, Guillemot F. Molecular mechanisms underlying cell fate specification in the developing telencephalon. Curr Opin Neurobiol. 2002; 12:26–34. [PubMed: 11861161]
34. Bareyre FM, Kerschensteiner M, Misgeld T, et al. Transgenic labeling of the corticospinal tract for monitoring axonal responses to spinal cord injury. Nat Med. 2005; 11:1355–60. [PubMed: 16286922]
35. Chan CH, Godinho LN, Thomaidou D, et al. Emx1 is a marker for pyramidal neurons of the cerebral cortex. Cereb Cortex. 2001; 11:1191–8. [PubMed: 11709490]
36. Bannerman PG, Hahn A, Ramirez S, et al. Motor neuron pathology in experimental autoimmune encephalomyelitis: studies in THY1-YFP transgenic mice. Brain. 2005; 128:1877–86. [PubMed: 15901645]
37. Gran B, Zhang GX, Yu S, et al. IL-12p35-deficient mice are susceptible to experimental autoimmune encephalomyelitis: evidence for redundancy in the IL-12 system in the induction of central nervous system autoimmune demyelination. J Immunol. 2002; 169:7104–10. [PubMed: 12471147]
38. Franklin, KB.; Paxinos, G. The mouse brain in stereotaxic coordinates. San Diego, CA: Academic Press; 1997.
39. Ray SK, Schaecher KE, Shields DC, et al. Combined TUNEL and double immunofluorescent labeling for detection of apoptotic mononuclear phagocytes in autoimmune demyelinating disease. Brain Res Brain Res Protoc. 2000; 5:305–11. [PubMed: 10906497]
40. Guo F, Ma J, McCauley E, et al. Early postnatal proteolipid promoter-expressing progenitors produce multilineage cells in vivo. J Neurosci. 2009; 29:7256–70. [PubMed: 19494148]

41. Schneider CA, Rasband WS, Eliceiri KW. NIH Image to Image J: 25 years of image analysis. Nature Methods. 2012; 9:671–5. [PubMed: 22930834]
42. Sailer M, Fischl B, Salat D, et al. Focal thinning of the cerebral cortex in multiple sclerosis. Brain. 2003; 126:1734–44. [PubMed: 12805100]
43. Lazeron RH, Langdon DW, Filippi M, et al. Neuropsychological impairment in multiple sclerosis patients: the role of (juxta)cortical lesion on FLAIR. Mult Scler. 2000; 6:280–5. [PubMed: 10962549]
44. Chiaravalloti ND, DeLuca J. Cognitive impairment in multiple sclerosis. Lancet Neurol. 2008; 7:1139–51. [PubMed: 19007738]
45. Filippi M, Rocca MA, Barkhof F, et al. Association between pathological and MRI findings in multiple sclerosis. Lancet Neurol. 2012; 11:349–60. [PubMed: 22441196]
46. Mangiardi M, Crawford DK, Xia X, et al. An animal model of cortical and callosal pathology in multiple sclerosis. Brain Pathol. 2011; 21:263–78. [PubMed: 21029240]
47. Argaw AT, Asp L, Zhang J, et al. Astrocyte-derived VEGF-A drives blood-brain barrier disruption in CNS inflammatory disease. J Clin Invest. 2012; 122:2454–68. [PubMed: 22653056]
48. Bannerman P, Hahn A. Enhanced visualization of axonopathy in EAE using thy-1YFP transgenic mice. J Neurol Sci. 2007; 1–2:23–52.
49. Jones MV, Nguyen TT, Deboy CA, et al. Behavioral and pathological outcomes in MOG 35-55 experimental autoimmune encephalomyelitis. J Neuroimmunol. 2008; 199:83–93. [PubMed: 18582952]
50. Lee E, Chanamara S, Pleasure D, et al. IFN-gamma signaling in the central nervous system controls the course of experimental autoimmune encephalomyelitis independently of the localization and composition of inflammatory foci. J Neuroinflammation. 2012; 9:7. [PubMed: 22248039]
51. Brown DA, Sawchenko PE. Time course and distribution of inflammatory and neurodegenerative events suggest structural bases for the pathogenesis of experimental autoimmune encephalomyelitis. J Comp Neurol. 2007; 502:236–60. [PubMed: 17348011]
52. Bö L, Vedeler CA, Nyland H, et al. Intracortical multiple sclerosis lesions are not associated with increased lymphocyte infiltration. Mult Scler. 2003; 9:323–31. [PubMed: 12926836]
53. Kutzelnigg A, Faber-Rod JC, Bauer J, et al. Widespread demyelination in the cerebellar cortex in multiple sclerosis. Brain Pathol. 2007; 17:38–44. [PubMed: 17493036]
54. Yang G, Parkhurst CN, Hayes S, et al. Peripheral elevation of TNF-alpha leads to early synaptic abnormalities in the mouse somatosensory cortex in experimental autoimmune encephalomyelitis. Proc Natl Acad Sci U S A. 2013; 110:10306–11. [PubMed: 23733958]
55. Vercellino M, Merola A, Piacentino C, et al. Altered glutamate reuptake in relapsing-remitting and secondary progressive multiple sclerosis cortex: correlation with microglia infiltration, demyelination, and neuronal and synaptic damage. J Neuropathol Exp Neurol. 2007; 66:732–9. [PubMed: 17882017]
56. Wegner C, Esiri MM, Chance SA, et al. Neocortical neuronal, synaptic, and glial loss in multiple sclerosis. Neurology. 2006; 67:960–7. [PubMed: 17000961]

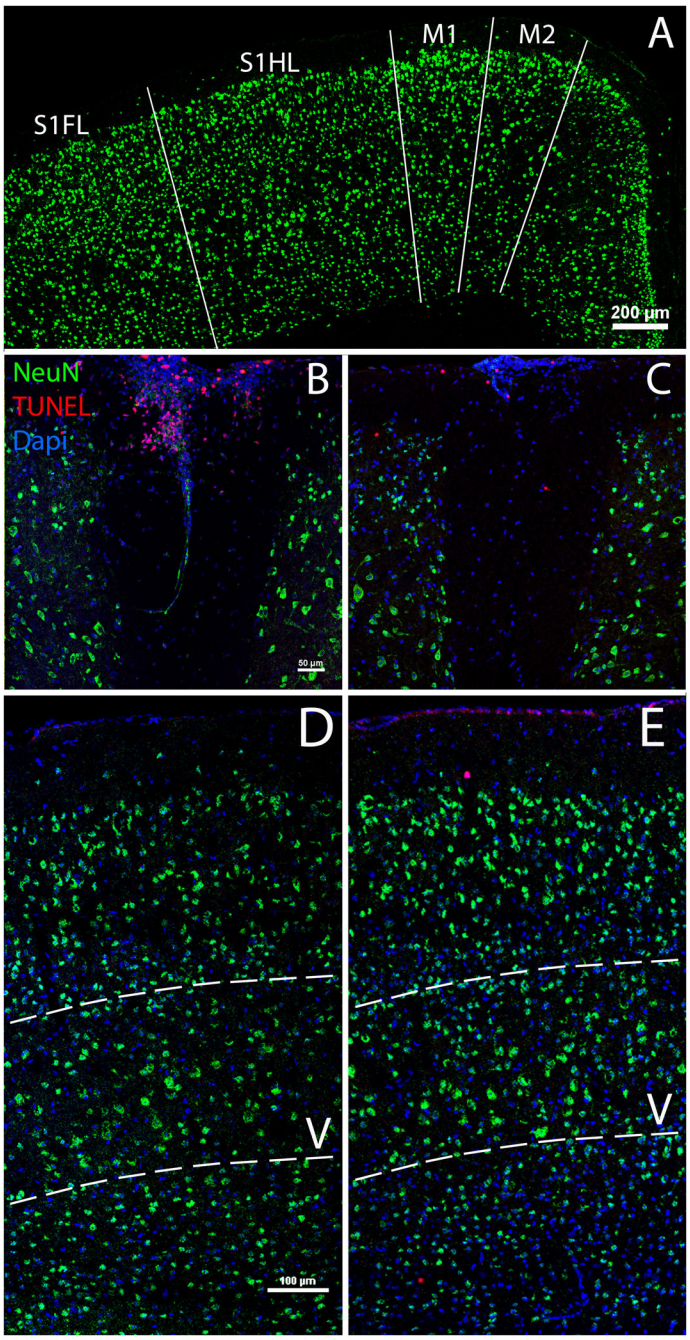

Figure 1.

Immunofluorescence showing NeuN-positive (green) regions of interest investigated in the study and absence of TUNEL-positive (red) cells in layer V of the neocortex in contrast to the spinal cord. (**A**) NeuN-positive neurons in the motor strip of a control (CFA) mouse (scale bar = 200 µm). (**B, C**) TUNEL-positive cells are present in inflammatory lesions in the dorsal funiculus of day (D)14 and D35 of myelin oligodendrocyte glycoprotein-peptide induced experimental autoimmune encephalomyelitis (MOGp-EAE) mice (scale bar = 50 µm). (**D, E**) Absence of TUNEL-positive cells in layer V (delineated by white dashes) of the

S1HL region of the motor strip in corresponding D14 and D35 MOGp-EAE mice (scale bar = 100 μm). There is a paucity of submeningeal inflammatory infiltrates in the cortex compared to the typical lesions associated with blood vessels in the spinal cord. Nuclei are labeled with DAPI (blue). M1, primary motor cortex; M2, secondary motor cortex; S1HL, primary somatosensory, hind limb region; S1FL, primary somatosenory, forelimb region.

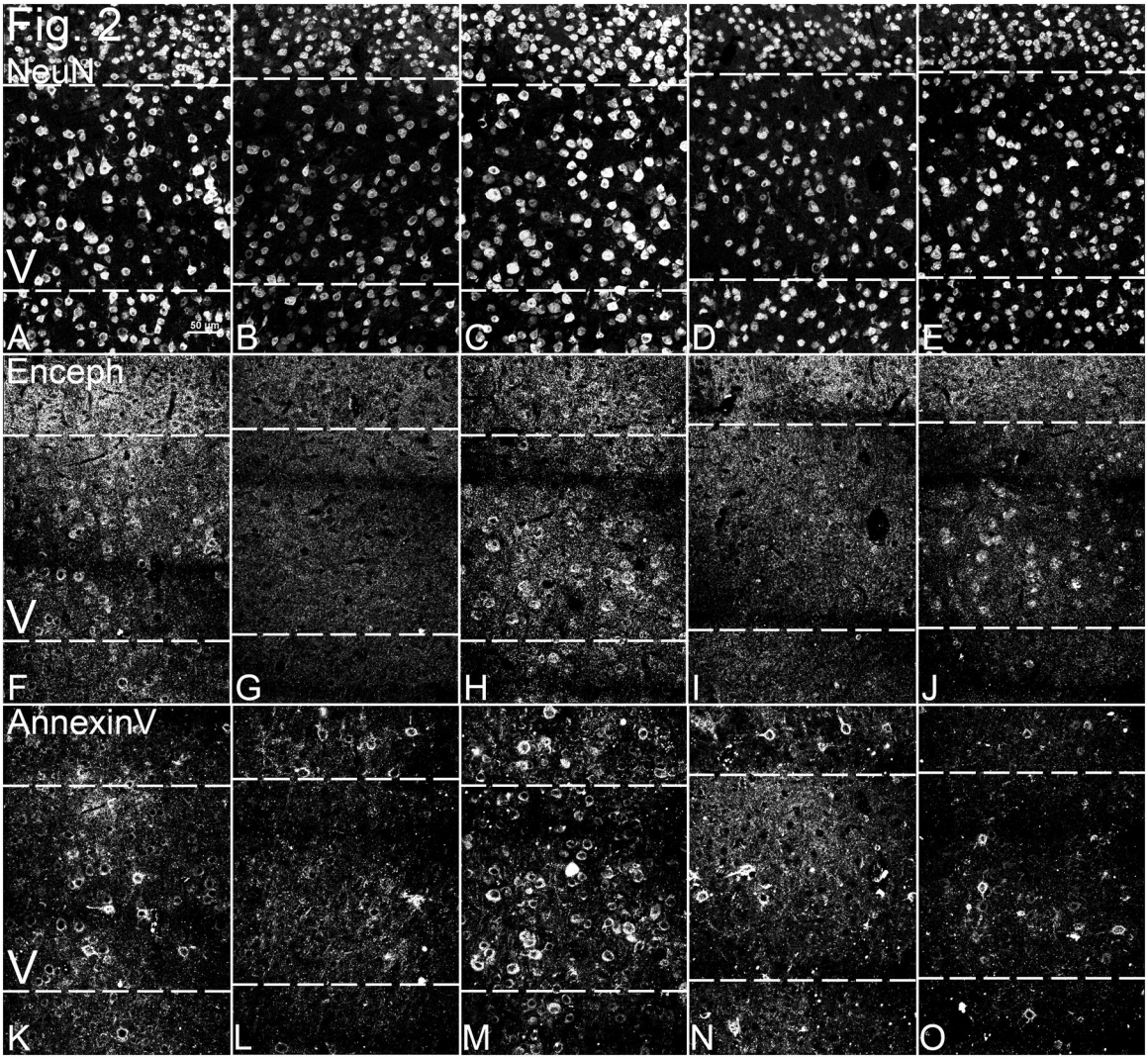

Figure 2.

(**A–O**) Immunofluorescence confocal micrographs showing perikaryal expression of NeuN (**A–E**), encephalopsin (**F–J**) and annexin V (**K–O**) immunoreactivity in the S1HL region of the motor strip of control (CFA) (**A, F, K**) and mice at day (D)14 (**B, G, L**), D21 (**C, H, M**), D35 (**D, I, N**) and D100 (**E, J, O**) with myelin oligodendrocyte glycoprotein-peptide (MOGp) induced experimental autoimmune encephalomyelitis. In these coronal paraffin sections of layer V frontal neocortex (delineated with dashed lines), decreased expression of NeuN, encephalopsin and annexin V is seen at D14 post-MOGp-inoculation vs. control tissue. There is a second dramatic decrease for encephalopsin at D35 (**I**). The decreases in NeuN and encephalopsin expression appear to be reversible because the level of expression of all these markers rebounded to control levels at D100 (**E, J**). Each micrograph represents stacked 0.4 μm optical sections from 30-μm-thick paraffin sections. For each marker, images were captured using the same laser power and voltage/offset settings at each time-point (scale bar = 50 μm).

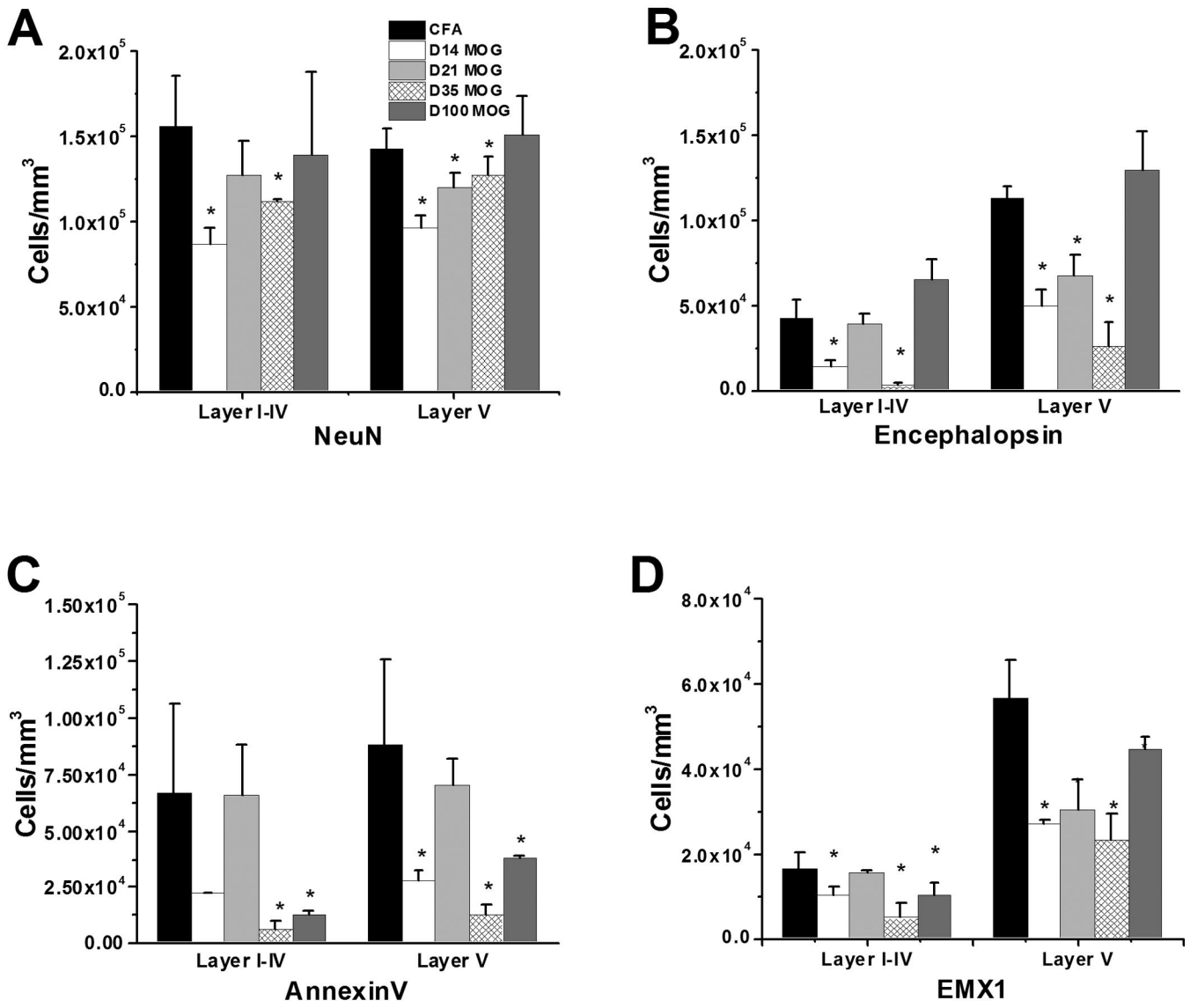

Figure 3.

(**A–D**) Bar histograms quantifying the numbers of NeuN (**A**), encephalopsin (**B**), annexin V (**C**), and Emx1 (**D**) in Layer V and Layers I to IV in the M1, M2, and S1HL regions of the motor strip of control (CFA) mice and mice with MOGp-EAE at D14, D21, D35, and D100 after MOGp vaccination. Data were obtained using nonbiased stereology. Data are mean ± SEM, n = 3, * $p < 0.05$ versus control values.

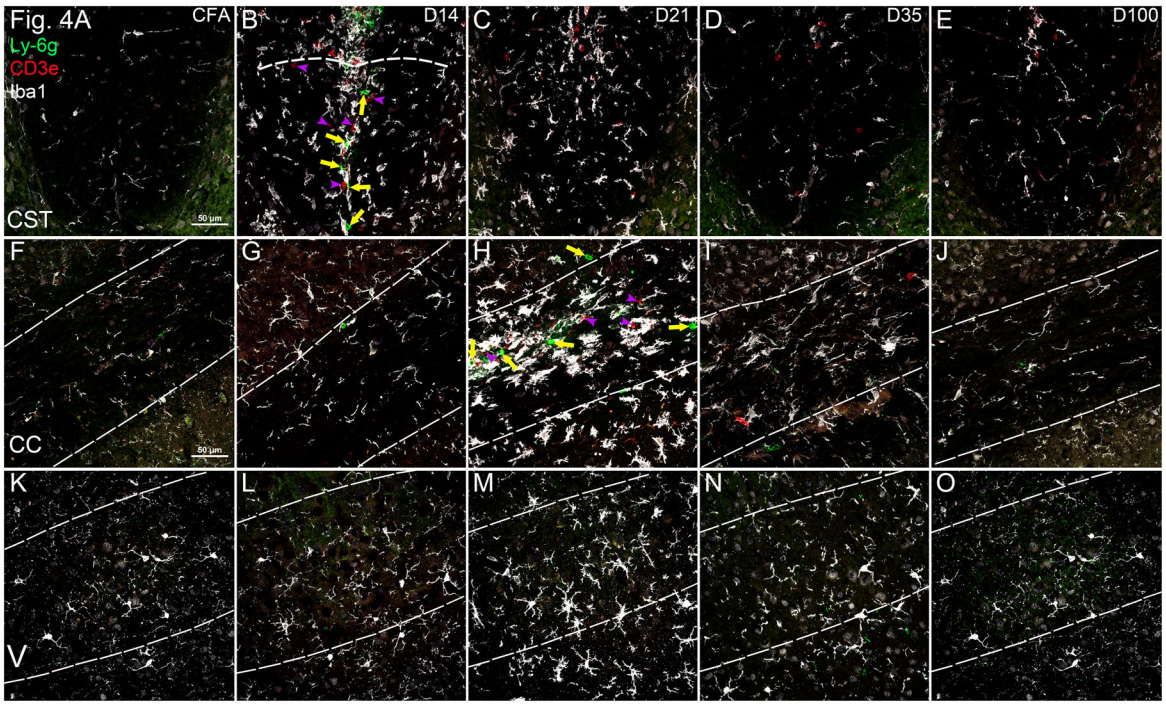

Figure 4.

(**A–O**) Triple labeled confocal micrographs showing the presence of Ly6G-positive neutrophils (green with yellow arrows), CD3-positive T cells (red with purple arrowheads) and Iba1-positive microglia/macrophages (white) in the corticospinal tract (CST) (**A–E**), corpus callosum (CC) (**F–J**) and layer V in the S1HL region of the motor cortex (**K–O**) in control (CFA) (**A, F, K**) and day (D)14 (**B, G, L**), D21 (**C, H, M**), D35 (**D, I, N**), and D100 (**E, J, O**) mice with myelin oligodendrocyte glycoprotein-peptide induced experimental autoimmune encephalomyelitis (MOGp-EAE). Within the CST (ventral aspect of the dorsal funiculus, delineated by area below dashed line in [**B**]), inflammatory infiltrates typically include neutrophils, T cells and microglia/macrophages by D14. Within both layer V of the cortex and the underlying CC, an overt inflammatory response was absent at D14 but evident at D21 post-MOGp immunization; although neutrophils and T cells were present in the CC, they were largely absent within the cortex. There are differences in the morphology of Iba1-positive cells in the cortex, i.e. ramified appearance vs. those in the CC (with both amoeboid and ramified morphologies). Scale bar = 50 μm.

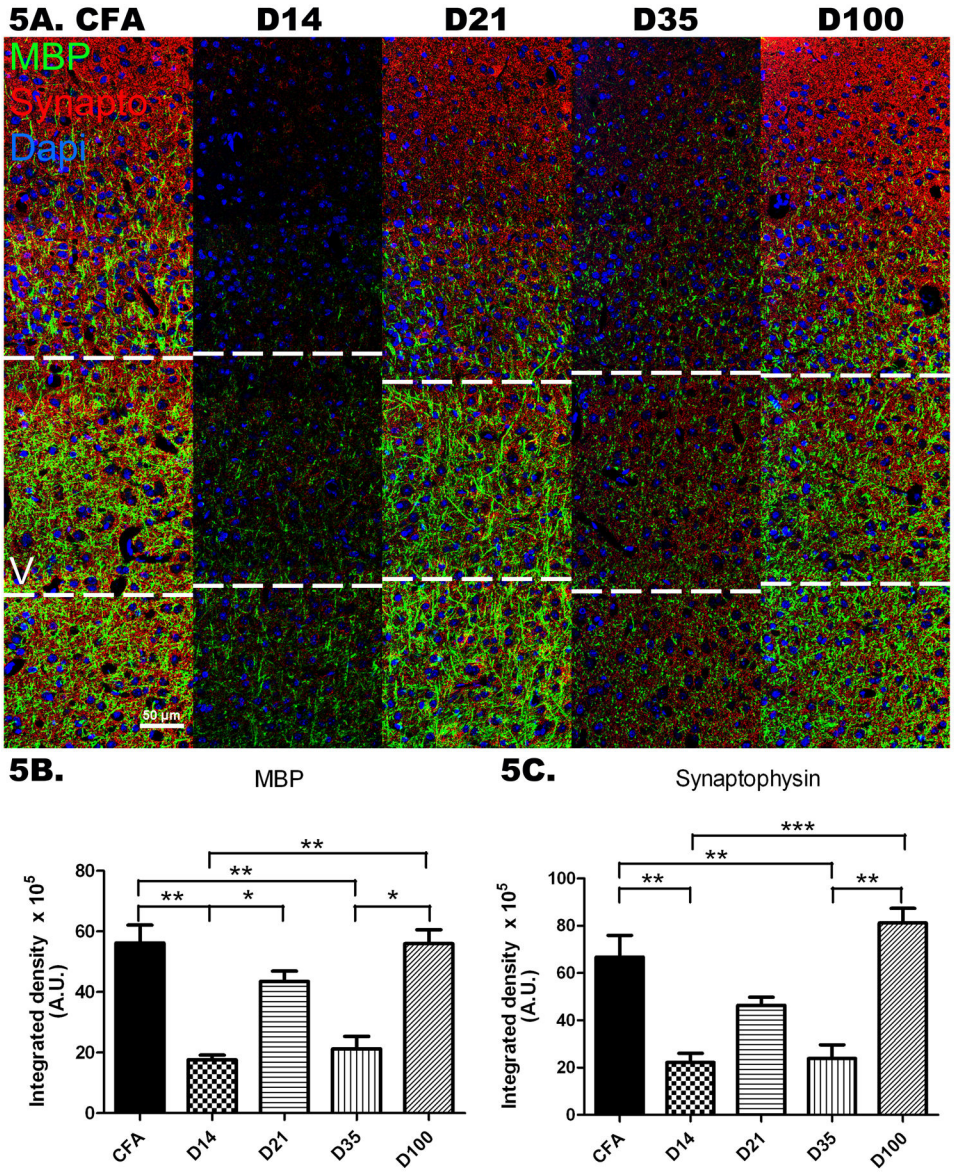

Figure 5.

(**A**) Immunofluorescence panels showing myelin basic protein (MBP)-positive (green) and synaptophysin-positive (red) cells in layers I through VI (layer V delineated by white dashes) in the S1HL region of the motor cortex in control (CFA) mice, and in day (D)14, 21, 35 and 100 mice with myelin oligodendrocyte glycoprotein-peptide induced experimental autoimmune encephalomyelitis (MOGp-EAE). Nuclei are labeled with DAPI (blue, scale bar = 50 µm). **(B, C**) panels showing relative integrated density panels in arbitrary units (A.U.) for MBP and synaptophysin immunolabeling in CFA and D14, 21, 35 and 100 mice with MOGp-EAE in S1HL cortical regions depicted in **A.** (Bars indicate mean values ± SE; asterisks denote levels of significance; *p ≤ 0.05; **p ≤ 0.01; ***p ≤ 0.001). There are transient decreases in immunolabeling at D14 and D35 compared to both CFA and D100 MOGp-EAE mice (**A–C**).

Table 1

Table Primary Antibodies Used for Immunohistochemistry

Antigen	Processing	Type, Source, Dilution
Annexin V	P (AR Na Citrate)	Goat polyclonal anti-Annexin V (c-20), Santa Cruz Biotechnology, Santa Cruz, CA, 1:20
Caspase-3	Fr/P (AR Na Citrate)	Rabbit mAb anti-Cleaved Caspase-3, Cell Signaling, Millipore, Billerica, MA, 1:400
CD 11b	Fr	Rat anti-mouse CD11b, BD Biosciences, San Jose, CA1:100
Emx 1	P (AR Na Citrate)	Rabbit polyclonal anti-Emx1, AbCam, Cambridge, MA1:200
Encephalopsin	P (AR Na Citrate)	Rabbit polyclonal anti-Encephalopsin, AbCam, 1:200
GFAP	Fr/P (AR Na Citrate)	Rat anti-GFAP, gift of V. Lee, University of Pennsylvania, Philadelphia, PA, 1:50
Iba-1	Fr/P (AR Na Citrate)	Rabbit polyclonal anti-Iba1, Wako, Mountain View, CA 1:500
Myelin Basic Protein (MBP)	P (AR Na Citrate)	Rat anti-MBP, gift of V. Lee, 1:2
NeuN	Fr/P (AR Na Citrate)	Mouse anti-NeuN, Millipore, 1:500
Synaptophysin	P (AR Na Citrate)	Rabbit monoclonal anti-Synaptophysin, Millipore, 1:200

Fr, frozen section; P, paraffin section; FR/P, frozen and/or paraffin; AR, antigen retrieval.

Fluorescent conjugated secondary antibodies were from Jackson ImmunoResearch (West Grove, PA) and were used at 1:500 or 1:1000. mAb, monoclonal antibody.